Validation of mesoscale precipitation in the NCEP reanalysis using a new grid-cell data set for the northwestern United States

Martin Widmann* and Christopher S. Bretherton

Department of Atmospheric Sciences
University of Washington
Seattle, Washington

submitted to *Journal of Climate* June 1998, revised April 1999

* *Corresponding author address*: Dr. Martin Widmann, Institute of Hydrophysics, GKSS Research Centre, D-21502 Geesthacht, Germany. E-mail: widmann@gkss.de

Abstract

Precipitation fields from the NCEP reanalysis are validated with high-resolution, gridded precipitation observations over Oregon and Washington. The NCEP reanalysis is thought of as a proxy for an ideal general circulation model that nearly perfectly represents the synoptic-scale pressure, temperature and humidity, but does not resolve the complex topography of this region. Our main goal is to understand how useful precipitation fields from such a model are for estimating temporal variability in local precipitation.

The gridded observations represent area-averaged precipitation on a 50 km grid and have daily temporal resolution. They are calculated with a newly developed scheme, which explicitly takes into account the effect of the topography on precipitation. This gridding method profits from the already existing, high-resolution climatologies for the monthly-mean precipitation in the United States, obtained from PRISM (Parameter-elevation Regressions on Independent Slopes Model), by using these climatologies for calibration. We also discuss the estimation of daily precipitation on scales as small as 4 km.

The reanalysis captures well precipitation amounts and month-to-month variability on spatial scales of about 500 km or 3 grid cells, which indicates a good performance of the precipitation parametrization scheme. On smaller spatial scales the NCEP reanalysis has systematic biases, which can be mainly attributed to the poor representation of the topography, but can nevertheless be used to reconstruct the temporal variability of local precipitation on daily to yearly time scales. This suggests that GCM precipitation might be a good predictor for statistical downscaling techniques.

1 Introduction

Changes in precipitation patterns associated with natural and anthropogenically induced climate variations have enormous ecological, societal and economic impacts. Our most sophisticated tool for understanding and predicting climate variability on seasonal to multi-decadal time scales is the atmospheric general circulation model (GCM), coupled to models of ocean circulation, land surface, and snow and ice cover.

A comprehensive verification of continental- to global-scale GCM-predicted precipitation patterns (Lau et al. 1996) was conducted during phase 1 of AMIP (Atmospheric Model Intercomparison Project). AMIP analyzed the performance of 29 atmospheric GCMs forced by observed sea surface temperature and sea ice conditions over a ten year period. The best current GCMs were found to have moderate skill in predicting the seasonal distribution of precipitation on continental scales (though there is considerable scatter between models). Most GCMs reproduced reasonably well the tropical interannual variability in precipitation associated with ENSO. In the extratropics the models had little skill in predicting interannual rainfall anomalies due to SST forcing, even in regions where such a correlation is observed. An analysis of river runoff indicated that 'it is premature to use them [GCMs] for climate studies related to continental-scale water balance'. Synoptic scales were not explicitly investigated by Lau et al. (1996), but a comparison of the mean precipitation patterns in different models based on their figures shows even larger differences on this scale. Osborne and Hulme (1998) used daily time series from several dozen stations in western Europe to evaluate mesoscale precipitation from 12 AMIP models with respect to seasonal mean precipitation, daily standard deviation, frequency of raindays and the mean precipitation intensity of raindays and found substantial differences between simulations and observations.

GCMs used for climate predictions currently have horizontal grid resolutions of 200-500 km and therefore the simulated precipitation depends not only on the large-scale atmospheric states but also strongly on parametrizations of sub-grid processes. Problems associated with both factors can contribute to unrealistically simulated precipitation and the assessment of their relative contributions is a field of ongoing research. Risbey and Stone (1996) analyzed the ability of several GCMs to simulate the large-scale processes which determine the regional precipitation in Northern California. The large-scale fields deviated strongly from the observations, even if the GCMs were driven by observed ocean boundary conditions and run at resolutions as high as T106. Leung and Ghan (1999) compared mesoscale precipitation from the CCM3 GCM, forced with observed SST and sea ice, with observed precipitation in the northwestern United States and found considerable, seasonally and regionally dependent discrepancies, which were also mostly attributable to differences between the simulated and the observed synoptic-scale circulation and the resulting differences in moisture fluxes. Busuioc et al. (1999) demonstrated that regional-scale GCM precipitation and synoptic-scale flow may be consistent. They found that the ECHAM3 atmospheric GCM reproduces the observed link between European SLP and Romanian precipitation (in terms of canonical correlation patterns) in winter and partially in fall and spring. A similar result was obtained by Osborn et al. (1999), who showed that the observed relations between precipitation over the United Kingdom and the local geostrophic flow strength, vorticity and direction are well simulated by the HadCM2 GCM. However, Wilby and Wigley (1999) found the HadCM2 GCM less satisfactory in reproducing the observed correlations between daily precipitation over six regions in the United States and a variety of different atmospheric predictor variables.

In mountainous or coastal regions precipitation and its partitioning into rain vs. snow can vary drastically on the mesoscale, i.e. scales from a few km to a few hundreds km, which cannot be resolved by current GCMs. Predicting how mesoscale precipitation will change in association with large-scale climate variations, or 'downscaling', is very important to regional climate change impact assessment. One method for downscaling is to apply empirically-derived statistical relations between mesoscale precipitation patterns and larger-scale atmospheric fields to GCM-simulated fields. Another more computationally intensive and less tested approach is to use precipitation patterns from a high-resolution regional numerical forecast model, driven by GCM-simulated fields used as boundary conditions, over a representative subset of the time interval to be predicted. If statistical methods are employed, a key issue is the choice of the predictor fields. Many researchers have discounted the GCM precipitation field in favor of fields that represent the synoptic-scale circulation, which they perceive to be more reliably simulated. However, some of the studies discussed in the previous paragraph indicate that, for some models and regions, GCM-simulated precipitation may realistically represent precipitation changes associated with changes in the synoptic-scale circulation, and hence might be a good predictor in statistical downscaling algorithms.

In this paper, we explore whether changes in precipitation derived from a GCM can be a good representation of the variability of area-averages even in regions of complex terrain. Specifically, our goals are (1) to derive a fifty year long, gridded, daily data set of observed mesoscale precipitation patterns in a coastal, mountainous region, namely the states Oregon and Washington in the northwestern United States, and (2) to compare this data set with the NCEP/NCAR reanalysis (National Center for Environmental Prediction / National Center for Atmospheric Research; Kalnay et al. 1996). In the reanalysis, a state-of-the-art global forecast model is used to assimilate observed atmospheric data in a physically consistent way. The observations entering the reanalysis include pressure, temperature and humidity taken from radiosonde and satellite measurements and surface networks. The model precipitation field is calculated according to the model physics and parametrizations, and is not adjusted to observations. Roughly speaking, we think of the reanalysis as an ideal GCM, in which the time-varying, synoptic-scale pressure, temperature and humidity is accurately represented. The resolution of the forecast model used for the reanalysis (T62, about 2° or 200 km over our analysis domain) is somewhat higher than what is currently customary in climate change and climate variability experiments, but is likely to be typical in a few years.

Mo and Higgins (1996) compared global precipitation fields and other components of the hydrological cycle modeled by the NCEP and NASA reanalyses with satellite and station observations from the period 1986-1992 and found significant regional biases between both reanalyses and the observations. Higgins et al. (1996) used about 2800 daily precipitation records in the conterminous United States to examine precipitation from the NCEP and the NASA reanalyses for May 1985-1989. The skills of both reanalyses exhibit large regional differences. Over Oregon and Washington the biases are moderate and the correlations of reanalyzed and observed daily values are high, in particular for the NCEP reanalysis and along the coast (up to 0.8). Janowiak et al. (1998) compared global precipitation fields from the NCEP reanalysis with 2.5° resolution monthly precipitation fields from the Global Precipitation Climatology Center (GPCC, Huffman et al. 1997) for the period 1988-1995. Although the GPCC data and the spatial resolution of the maps in Janowiak et al. (1998) are not optimal for a regional analysis, the study indicates that the correlations between observed and reanalyzed monthly means are higher than 0.7 over most parts of Oregon and Washington, but that the NCEP reanalysis is too wet in the eastern parts of this region. Again, the global maps for mean annual differences and correlations between observations and reanalysis show large spatial variability. GPCC data for the years 1988-1993 were also used by Stendel and Arpe (1997) to validate precipitation fields from different reanalyses (NCEP, ECMWF, NASA). Their maps of average seasonal precipitation indicate for the northwestern United States a relatively good agreement of the reanalyses among each other and with the observations. Gutowski et al. (1997) compared the convergence of water moisture transport from the NCEP reanalysis over two large river basins in the central United States with observed river discharges in the years 1984-1993. For time scales long enough to exclude major effects of water storage, water input from the atmosphere should match the streamflow, but substantial biases were found in both basins. The temporal variability of the two quantities is in useful correspondence on several-day to interannual time scales.

Our validation of reanalyzed precipitation in a mountainous region requires that the area means against which the comparison is made are constructed in a especially careful way. (Note that, in accordance with the prevailing understanding, we assume that the simulated precipitation represents an area mean over the entire grid cell. An alternative view is discussed in Skelly and Henderson-Sellers 1996.) The main problem in estimating the area mean from records at the observation sites stems from their non-representative distribution with respect to height, combined with the strong effect of topography on precipitation. We address this issue by presenting a new interpolation scheme for estimating areally averaged precipitation in mountainous terrain. The method builds on a modified Shepard interpolation algorithm (Shepard 1968, 1984) and yields daily fields that are consistent with the elevation-bias-corrected, monthly PRISM climatologies (Parameter-elevation Regressions on Independent Slopes Model) developed by Daly et al. (1994, 1997). Using 522 station records from Washington and Oregon, we derive estimates of area-averaged, daily precipitation for the period 1949-1994 over grid cells with a size of about 50 km $\times$ 50km. This resolution is comparable to the station density and finer than what is needed for the model validation presented here. Its high resolution makes this gridded precipitation data set suitable for other potential applications, for instance tests of hydrological (streamflow) models using historical data, statistical downscaling, validation of regional numerical models and climatological studies.

2 Gridded daily precipitation

Individual precipitation events as well as long-term means show a high spatial variability on scales as small as few hundred meters. Over mountainous terrain the spatial structure of precipitation is particularly complex and has been investigated since the early years of mountain meteorology. For example Raulin (1879) was one of the first studies demonstrating the various 'climatic spheres' influencing the European Alps. Measurements for individual precipitation events are usually inadequate to fully resolve the spatial variability and most studies focus on long-term mean precipitation, often with a particular interest in vertical precipitation gradients. Comprehensive listings of such studies can be found in Daly et al. (1994) and Frei and Schär (1998).

Note however that since we are dealing with a field given on a 2-dimensional surface embedded in 3-dimensional space, horizontal and vertical gradients are not well defined a priori and some clarification is needed if these notions are used. The usual approach to define a vertical gradient is to choose an area of interest, then to assume the horizontal gradients within that region to be small and attribute the point-to-point variations of precipitation to a systematic height dependence and additional random residuals. It was found that variations of mean precipitation over large mountain ranges cannot be adequately described by one overall vertical gradient. Examples are areas in the central Alps where the lowest precipitation in the whole Alpine region is found despite the high elevation, or the large precipitation differences between the west and the east side of the Cascade Mountains in the northwestern United States. It is more appropriate to divide a mountain range in subregions, with a horizontal precipitation variation accounting for the differences in the mean precipitation within these subregions. Precipitation-height relations defined separately for each of these subareas typically reveal a considerable spatial and seasonal dependence. Furthermore these relations are not always linear.

Grid-cell precipitation data sets can be compiled accurately by averaging the observational records, if the station density is high enough to resolve the major orographic effects. This is the case for most countries in the European Alps, where about 1 station per 100 km^2 is typically available (e.g. about 500 stations in Switzerland, which is slightly more than twice the size of New Jersey). Note however that the observation sites tend to be located at lower elevations, thus introducing a systematic bias in the data. Such a direct gridding approach was used by Frei and Schär (1998), who collected a comprehensive set of more than 6800 daily station records for the whole Alpine region (see also http://map.ethz.ch/rr_clim.htm). From these records they calculated daily gridded fields for the period 1971-1990 with a resolution of about 25 km. In order to account for the irregular spatial distribution of the observation sites, they employed a distance- and direction-weighted interpolation scheme, which is based on Shepard (1968, 1984). A comparison of their results with the coarser global climatology of Legates and Willmott (1990) and with the Greater European Climatology from the Climate Research Unit (University of East Anglia, UK, see Hulme et al. 1995) revealed some substantial differences, showing the need for high-resolution precipitation data sets over mountainous terrain.

In contrast to the Alpine region, the daily precipitation data sets for the United States have a considerably lower data density, on the order of 1 station per 1000 km^2, and are particularly sparse in mountainous regions. Therefore a direct gridding approach will presumably lead to large errors and should be replaced by a method that includes some representation of the topography and its effect on precipitation. We address this problem by calibrating our gridded daily data with the long-term (1961-1990), very high resolution, monthly precipitation climatologies for the United States obtained from PRISM (Parameter-elevation Regressions on Independent Slopes Model, Daly et al. (1994, 1997), see also http://www.ocs.orst.edu/prism/prism_new.html). In principle this idea was described and employed in Nijssen at al. (1997). For our work it was further refined by replacing the use of Thiessen-polygons by a modified Shepard scheme and by an improved handling of missing values (both issues are discussed in section 2.3).

2.1 PRISM precipitation climatologies

PRISM uses local, linear precipitation-height regressions and a digital elevation model (DEM) with a resolution of about 4 km x 4 km (Fig. 1). To determine the precipitation value for a certain grid point in the DEM, long-term mean observations within a search radius around the grid point (typically 50-100 km, depending on the data density) are entered into a weighted linear regression. Observations are weighted based on several factors, including distance, elevation, mesoscale slope orientation (binned into eight compass directions), coastal proximity, and vertical placement in relation to the planetary boundary layer (i.e. stations within an estimated boundary layer tend to be grouped together). The analysis is done separately for every month of the year. By means of this local regression the long-term mean monthly precipitation for every DEM cell is determined. PRISM is based on several climate data sets: (i) the National Climatic Data Center (NCDC)

1961-1990 normals data set (CLIM-81) observed by the National Weather Service Cooperative Climate Network; (ii) the National Resources Conservation Service SNOTEL (SNOwpack TELemetry) network data set; and (iii) supplemental data sets submitted by the individual state climatologists or regional climate centers.

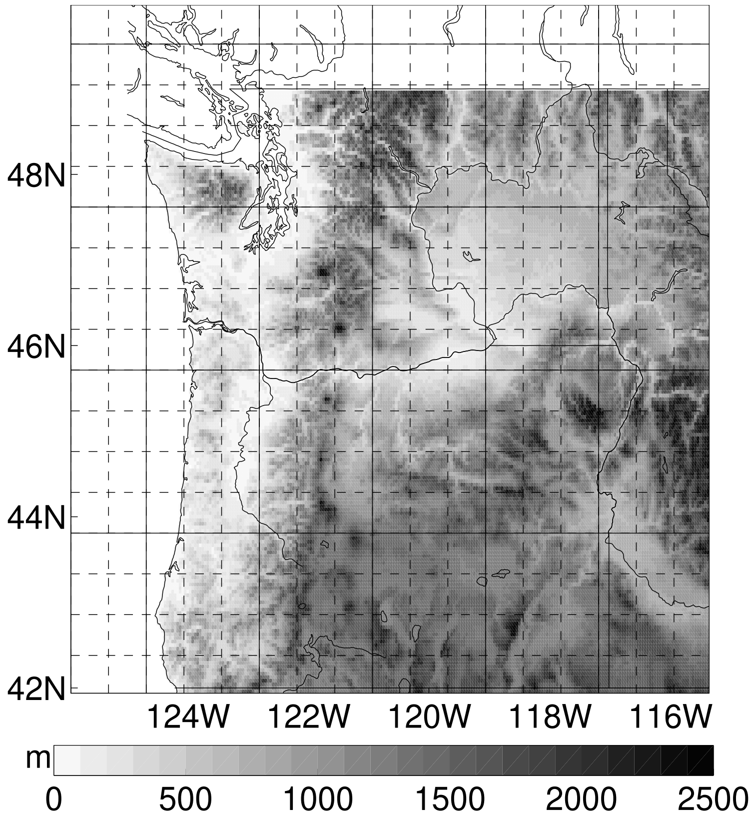

Figure 1: Topography of the northwestern United States as given by the 4 km $\times$ 4 km digital elevation data set used for PRISM. Also shown is the grid for the precipitation data set (dashed lines, resolution 52.5 km (lat) $\times$ 50 km (lon)), the Gaussian grid used in the NCEP reanalysis (solid lines), and coastlines, major rivers and borders of the states Oregon and Washington.

Daly et al. (1994) compared PRISM to other models (e.g. (co)-kriging) and found it well suited for the estimation of areal precipitation over mountainous terrain. Recently an alternative method to incorporate elevation as a predictor variable for (global) climatologies was used by New et al. (1999), who employed three-dimensional splines to describe the dependence of several atmospheric fields including precipitation on all three spatial directions. However, the applicability of this approach to high-resolution precipitation climatologies has yet to be tested. The limitations of PRISM stem from the linear assumption (although the regression slope is allowed to vary with elevation), the choice of the domains for the regressions, i.e. the distinction between horizontal and vertical gradients, the choice of the spatial scale used for the regressions, and the fact that regressions must sometimes be used for elevations beyond the range given by the observation sites. All these problems were carefully investigated prior to the formulation of PRISM and the selection of model parameters. PRISM also includes a post-processor to avoid unrealistic large gradients between adjacent areas. Errors of the PRISM climatologies are quantitatively discussed in Daly et al. (1994). Besides calculating prediction intervals for the local regressions, they performed a cross-validation by excluding some stations from the model fitting and using them to test the PRISM estimates. Typical errors (for Oregon) are a bias below 5% and a mean absolute error below 15%. Note however that the latter error generally decreases if the PRISM fields are averaged on a coarser grid, as will be done in our analysis.

An additional error, which is not corrected in the PRISM climatologies and not captured by the abovementioned numbers, stems from the well known fact that precipitation measurements are affected by systematic undercatches (Neff 1977; Sevruk 1982). The principal error source is the wind field deformation above the gage and hence these errors depend on the local wind speed, on the fallspeed of hydrometeors as well as on the gage type. Smaller contributions are due to wetting and evaporation losses. Legates and Willmott (1990) presented a global precipitation climatology which includes a correction for the estimated long-term means of the undercatches. Legates and DeLiberty (1993a,b) estimated time-dependent monthly biases of precipitation records in the Unites States. A map from Legates and DeLiberty (1993a) with the annual, long-term mean bias is reproduced in Groisman and Legates (1994). Annual-mean biases (1950-1987) in Washington and Oregon range from about 6% in the coastal regions to over 20% at high elevations; wintertime biases can exceed 30%.

These are substantial errors and therefore the estimation of area mean precipitation in mountainous regions should not only take into account the influence of the topography but also correct for the undercatch. A promising approach would be to first correct station records on a monthly basis and then apply a model like PRISM to the corrected monthly values or their long-term means. Currently no such product is available. Implementing and running PRISM requires considerable effort and was not a realistic option for us. This left us with two alternatives: to correct station records for the undercatch and use a standard gridding method, obtaining area means which would not explicitly include the effect of the terrain, or to use the PRISM climatologies to obtain a gridded field which accounts for the topography but not for the undercatch. We chose the second option since our main goal was to determine a series of daily fields which are consistent with a widely used, state-of-the-art climatology rather than establishing a new climatology. Moreover, the topography-induced biases (details are discussed below) are in general somewhat higher than the undercatch bias and therefore the former should be corrected first.

2.2 Daily precipitation data

The day-to-day variability in our grid-cell data set is derived from the 'Summary of the day' data from the NCDC. These consist of records from the National Weather Service and cooperators, corrected by NCDC's 'Validated Historical Daily Data' project, and are available on CD ROM (Earthinfo 1990). There are over 750 stations in Oregon and Washington, but, as can be seen in Fig. 2, only a small fraction of them was operating through the whole period 1949-1994. Included in our analysis are 522 stations (Fig. 3), that had enough observations to reliably estimate the long-term mean precipitation (details are discussed later). The actual number of stations within this subset reporting no more than 10 missing days for any given year is depicted in Fig. 4. The average over the whole period is 327. Note that the long-term monthly means of our gridded data are based on a higher number of stations, since they are given by the PRISM climatologies.

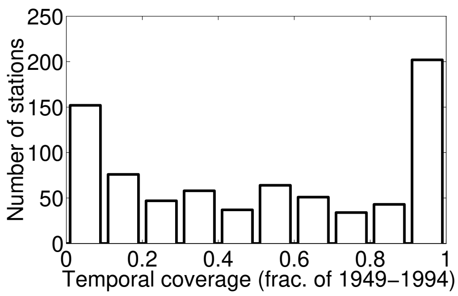

Figure 2: Number of NCDC precipitation stations in Oregon and Washington as a function of record length, which is given as a fraction of the whole period 1949-1994.

2.3 Gridding method

The output grid (Figs. 1 and 3) is defined as a sub-grid of the Gaussian NCEP model grid, with 12 precipitation grid cells covering one NCEP grid cell. The resolution of the precipitation grid is about $0.48°$ (lat) $\times\, 0.62°$ (lon) or 52.5 km (lat) $\times$ 50 km (lon) at 45°N. There is an average of about 2 stations per grid cell and therefore grid-scale features are generally resolved by the stations, but sub-scale structures are not.

Our gridding scheme is based on a decomposition of the precipitation field $\psi(x, y, t)$ in its climatological mean $\overline{\psi}(x, y)$ and the pointwise ratios $\psi_r(x, y, t)$ of the daily patterns and this mean

$$\psi(x, y, t) = \psi_r(x, y, t) \cdot \overline{\psi}(x, y) \ . \tag{1}$$

A different climatology $\overline{\psi}(x, y)$ is used for every month, which is obtained by averaging the monthly PRISM fields over the 50 km cells of our output grid. The long-term monthly means of the estimated ratio field have to satisfy

$$\overline{\psi_r(x, y, t)} = 1 \ , \quad \forall\ x, y \ , \tag{2}$$

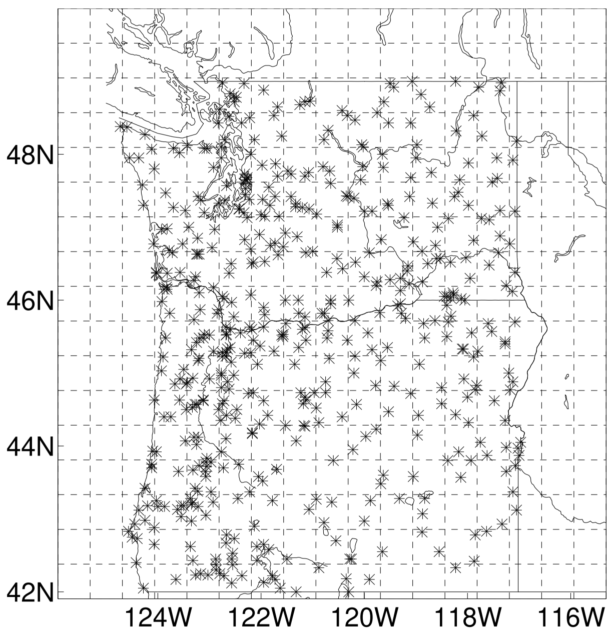

Figure 3: Locations of stations in Oregon and Washington that are used to calculate the temporal variability in the gridded precipitation data set. Dashed lines show the grid.

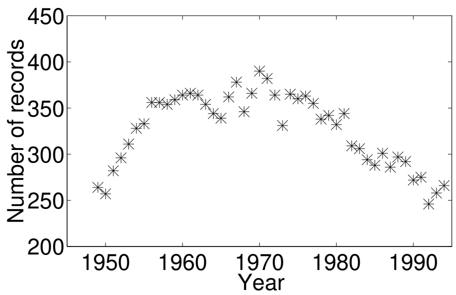

Figure 4: Number of NCDC precipitation records in Oregon and Washington as a function of the year. Only stations with no more than 10 missing days in a given year are taken into account.

with respect to the PRISM reference period 1961-1990. To obtain the values of $\psi_r(x, y, t)$ at the stations, we normalize the station records, separately for every month, such that their means with respect to 1961-1990 are equal to 1. The estimate of $\psi_r(x, y, t)$ on the 50 km grid is then calculated from these normalized station records and satisfies Eqn. 2. Details of the gridding scheme are discussed below. The final gridded field is calculated according to Eqn. 1 using the monthly climatologies.

We favor this approach over the more common decomposition of a field in its long-term mean and an additive anomaly $\psi(x, y, t) = \psi_a(x, y, t) + \overline{\psi}(x, y)$, mainly because only the multiplicative decomposition guarantees non-negative estimates for $\psi(x, y, t)$, and a dry field $\psi(x, y, t) = 0$ on days and in regions in which no station reported precipitation.

More general arguments for the multiplicative approach can be found if one assumes that precipitation series within an area about the size of the 50 km grid cells are approximately multiples of each other. Although the topographic effects on precipitation are complex and depend for example on wind speed and direction, the assumption of local proportionality seems closer to reality than the assumption that the anomalies are locally constant. To the extent that the local proportionality holds, one can argue that the true $\psi_r(x, y, t)$ is locally almost flat and therefore can be estimated with high precision from station data. A slightly less restrictive assumption is that locally the ratios of the variances can be approximated by

$$\frac{\overline{\psi_a^2(x_1, y_1, t)}}{\overline{\psi_a^2(x_2, y_2, t)}} \approx \left(\frac{\overline{\psi(x_1, y_1, t)}}{\overline{\psi(x_2, y_2, t)}} \right)^2 = k^2(x_1, y_1, x_2, y_2) \ . \tag{3}$$

We checked this assumption, separately for each month of the year, using 5 stations at Mt. Rainier, the highest mountain in Washington (the same stations which will be used in section 2.4). In all months the observations corroborate Eqn.3. Squared means and variances are highly correlated ($r = 0.92$ in January and $r > 0.95$ in all other months), but in some months there is a small positive offset for the variance. Consider now the mean squared errors obtained if we replace either the additive anomaly or the multiplicative ratio field at the location (x_2, y_2) by those at the location (x_1, y_1), i.e. consider $\Delta_a^2 = \overline{(\psi_a(x_2, y_2, t) - \psi_a(x_1, y_1, t))^2}$ and $\Delta_r^2 = \overline{\psi(x_2, y_2, t)}^2 \ \overline{(\psi_r(x_2, y_2, t) - \psi_r(x_1, y_1, t))^2}$. If Eqn.3 holds, it can be shown that

$$\frac{\Delta_r^2}{\Delta_a^2} = \frac{2\, k^2 \, (1 - r)}{1 + k^2 - 2rk} \ , \tag{4}$$

where r is the correlation between the two time series. This ratio is smaller than 1 for any correlation if $k < 1$, or for $k > 1/(2r - 1)$ and $r > 0.5$. Hence for highly correlated time series and for most values of k it is better to replace the true ratio rather than the true anomaly with that of neighbors. This indicates again that the ratio field is locally flat and well suited for being estimated from observations.

For those stations with missing data over the period 1961-1990, the station mean precipitation, which is required for the normalization of the records, has to be estimated. Following the so-called augmentation procedures used in hydrology (c.f. Vogel and Stedinger 1985), we use linear regressions with the best-correlated stations within a distance of 100 km. The regressions are based on monthly means and are performed separately for every month of the year, in order to account for seasonal differences in the relations between stations. For the calculation of correlation and regression coefficients the whole records from 1949-1994 are used. For each month of the year we require data from at least 8 common years to perform a regression, and in most cases this number is much higher. As many missing months as possible are substituted using the best-correlated neighbor station, then the second-best correlated station is used and so on. Our estimate for the long-term monthly station mean is given by the average of all observed or estimated monthly means in the period 1961-1990. If less than 27 of the 30 months in this period either are observed or can be estimated, the respective station record is not used for the gridding. The normalization of records with this estimate allows us to include observations which were available only for a relatively short time without introducing biases in ψ_r since all means are estimated with respect to the whole period.

Following Frei and Schär (1998), we use a modified version of the Shepard algorithm (Shepard 1968, 1984) to estimate area means of ψ_r from the normalized station records. The original Shepard scheme is formulated to obtain point estimates and for this purpose it includes an extrapolation of estimated precipitation gradients. Compared to other gridding methods, including kriging, the Shepard scheme generally performs equally well or better (c.f. discussion and references in Frei and Schär 1998, but note that the respective studies compare point estimates). The original Shepard scheme was used by the Global Precipitation Climatology Center (Deutscher Wetterdienst, Offenbach, Germany) to calculate gridded monthly precipitation totals for the earth's land surface with a two-step method (Rudolf et al. 1994, Rudolf et al. 1996). In the first step point estimates were calculated on a 0.5° grid and these were then averaged to obtain area-mean precipitation on a 1° grid (the highest weight was given to the 0.5° grid point at the center of the 1° cell, lower weights to those on the sides and on the corners). As discussed above, not only the long-term monthly means of $\psi_r(x, y, t)$ are homogeneous, but also the daily $\psi_r(x, y, t)$ do not, in most cases, have pronounced sub-grid extrema. Therefore, it is appropriate to estimate the area means of $\psi_r(x, y, t)$ directly from the normalized station records, using a weighted average of all records in the neighborhood of a grid cell, and to omit the intermediate step based on gradients and point estimates. If many stations per cell were available it might be better to estimate an area mean simply by averaging all records within a cell. However, if the cell length and the average station distance are comparable, as is the case here, the sampling error of the few stations within a cell is large and the area-mean estimate improves by taking into account records in the vicinity of the cell, as long as they are reasonably well correlated with the inner-cell values.

The weight w assigned to a station is expressed as

$$w = w_{rad} \cdot w_{dir} \ , \tag{5}$$

where the radial term w_{rad} depends only on the distance l to the center of the grid cell and the direction term w_{dir} takes into account the positions of all other stations within the search radius (for details see Shepard 1968). The direction term downweights stations which are located in the same direction from the center of the grid cell and gives higher weight to isolated stations. With our parameter setting, this effect is limited to a factor of 4. The radial term contains a maximal search radius L and has the form

$$w_{rad} = \frac{1}{2}\left(1 + \cos\frac{\pi\, l}{L}\right) \qquad \text{for } l \leq L \tag{6}$$

and $w_{rad} = 0$ otherwise. To calculate an area mean, we start with $L = 50$ km and, if less than 3 stations are found within the region, increase the search radius in 10 km intervals up to a maximum of 100 km.

At $l = L/2$ the radial weight decreases most rapidly and has dropped to 0.5 of its value at the center. Again, the use of a multiplicative rather than an additive decomposition of the precipitation field is advantageous because in the additive case a change in the search radius could include or exclude particularly wet or dry stations and thus lead to jumps in the grid-cell series. If normalized records are gridded, as in our case, this problem will not occur. The weights on each day add up to 1 but they may vary with time due to missing observations. This allows the long-term mean of the grid-cell average of ψ_r to deviate from 1 by typically 1%-2%. To ensure the consistency of the daily precipitation patterns with the PRISM climatologies, the gridded estimate of ψ_r is rescaled so that its monthly climatologies are exactly 1. Willmott et al. (1985) pointed out the importance of taking into account the curvature of the earth surface when formulating the Shepard scheme. We use a locally-spherical geometry (i.e. the geometry of the tangent plane) for the calculation of distances and angles, which means that we assume a flat earth only for distances up to the search radius L .

Osborn and Hulme (1997) recalled the fact that the temporal variance of an area mean is overestimated if only a few station records are averaged. According to Kagan (1966) the factor of overestimation is given by

$$\alpha = \frac{1 + (n-1)\,\bar{r}}{\bar{r}\,n} \;, \tag{7}$$

where n is the number of records and $\bar{r}$ is the true mean interstation correlation. As discussed in Osborn and Hulme (1997) the main problem with a correction of the variance is that $\bar{r}$ has to be reliably estimated from a few station records. We do not attempt a correction but merely use Eqn. 7 to obtain a rough estimate of the variance overestimation. For this purpose we assume that all station records used to calculate a grid-cell estimate have the same weight. Since at least 3 records are averaged and a realistic value for $\bar{r}$ within the search radius is 0.8, it follows that the overestimation is typically below 10%.

Fig. 5 shows a comparison of the long-term mean precipitation (1961-1990) obtained from the PRISM-calibrated grid-point series (which is identical to the mean of the monthly climatologies weighted by the length of the months) and the mean for the same period obtained from an uncorrected gridding approach using the modified Shepard scheme. For the latter, we applied the weights defined in Eqns. 5 and 6 and the abovementioned selection criterion for the search radius to the same set of 522 records we used in the PRISM-corrected gridding, but made no elevation or slope aspect corrections. The two climatologies differ by up to 50%, with the uncorrected climatology being generally drier to the west of the Coastal and Cascade Mountains and wetter in some regions to the east of these mountains. Another pronounced feature is the relatively high precipitation in the

Blue Mountains in north-eastern Oregon indicated by PRISM but not captured by the NCDC station records. These differences are mainly due to the PRISM-deduced correlation of precipitation with elevation, along with the preponderance of gauges located in valleys in these regions. For the same reason, the uncorrected estimate of total precipitation over Oregon and Washington in the period 1961-1990 is only 83% of that derived from the PRISM climatology. As one would expect, the uncorrected and PRISM-corrected time series of grid-average precipitation have very similar temporal variability; for 90% of the grid cells, the correlation between these two daily time series exceeds 0.95.

An example for the degree of correlation between the original station records and the gridded series is given in Fig. 6. The selected grid cell contains Mt. Rainier and the daily gridded values are compared to the records at the 5 stations which are closest to the center of the cell. The grid series is slightly influenced by a few additional, more distant stations, which are not included in this plot. As can be expected from the way the gridded values are calculated, there is a general, however not strict, decrease of the correlation between these values and the station records (r_{grid}) as the distance of the stations to the center of the cell increases. The strong effect of the topography on local precipitation is reflected in the relatively low correlation between the record at Electron Headworks and some of the other stations (r_{2493}). With the exception of White River RS, which has a shielded location to the east of Mt. Rainier, the station records reveal the well-known increase of precipitation with elevation.

The larger-scale correlation structure of daily precipitation is shown as a correlation map in Fig. 7. It is based on daily gridded precipitation series and uses a grid cell in northwestern Washington (Seattle area) as reference point. Correlations with the series at this cell exceed 0.7 in large areas to the west of the Cascade mountains, drop substantially to the east of the main crest to values around 0.4, but increase again slightly up to 0.5 further to the east. The latter is likely due to westerly flow situations and the associated orographically-induced precipitation, which affects both the western slopes of the Cascade mountains and the mountains in northeastern Washington (e.g. Kettle River Range and Calispell Peak, elevations around 2000 m). In the most distant region of southeastern Oregon the correlations with precipitation in the Seattle area are almost zero.

2.4 Estimation of local precipitation series

Some problems in hydrology and glaciology could be more effectively addressed if gridded daily precipitation data sets with resolutions higher than 50 km were available. For instance, a distinction between snow and rain, based on elevation-dependent temperature estimates, would be more precise if the resolution of the precipitation data were high enough to determine the amount of precipitation which had fallen at different elevations.

The limited station density in the Pacific Northwest restricts meaningful interpolation of station records to scales around 50 km, unless additional variables, for instance elevation,

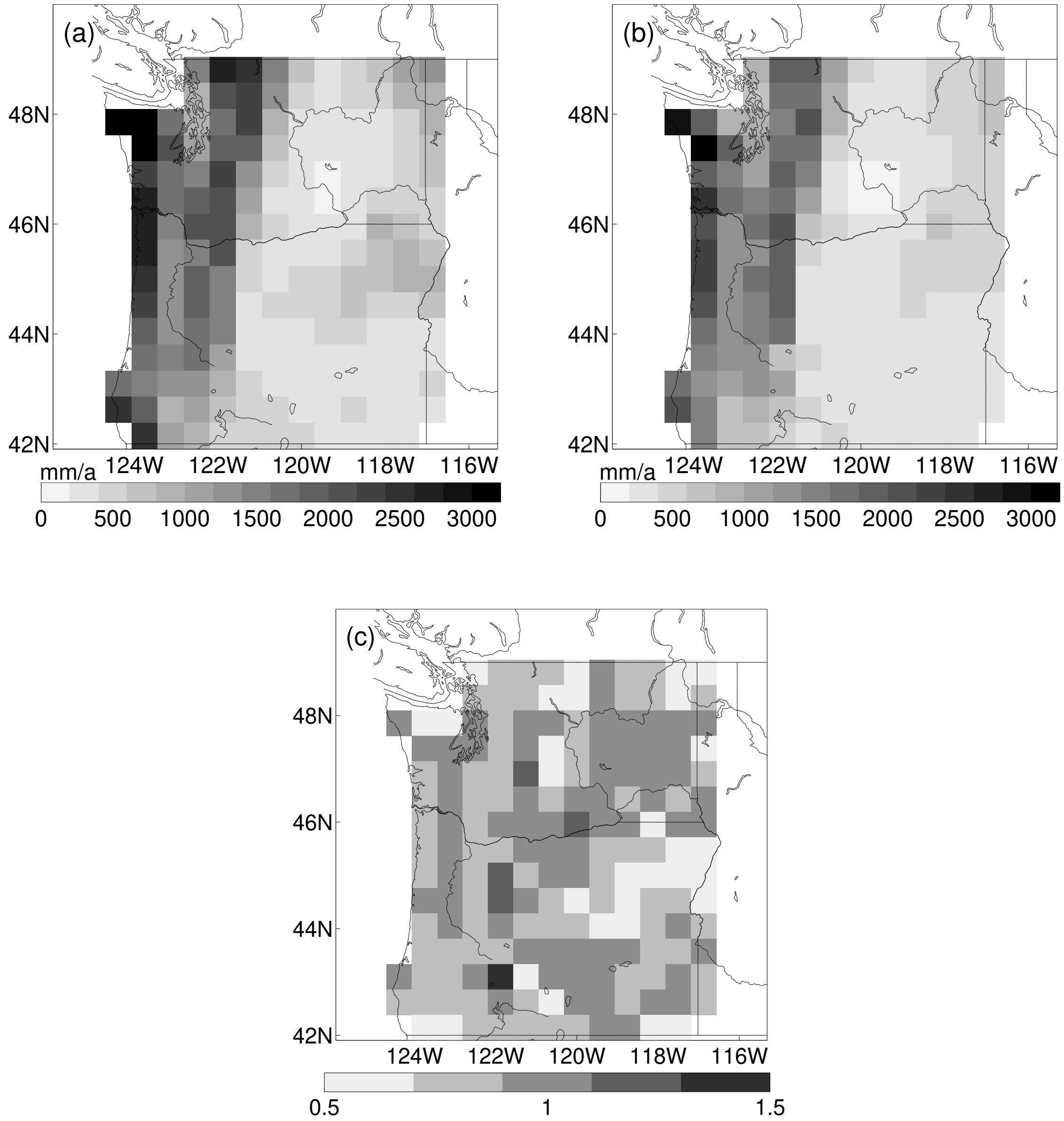

Figure 5: Comparison of mean precipitation (1961-1990) obtained from two different gridding methods (in mm/a): (a) Shepard gridding of normalized station records followed by a multiplication with the monthly PRISM climatologies; (b) Shepard gridding of original station records, i.e. no corrections for the effects of topography on precipitation were made; (c) ratio (b)/(a).

are explicitly accounted for. One approach (mentioned also on the PRISM web page) for a topography-based, high-resolution gridding of daily data would be to determine the PRISM regression lines separately for every day. From these one could deduce the fine structure of the daily precipitation, which can not be inferred from the station data only. However, this would require a substantial technical effort and introduce new conceptual problems related to parameter settings, design of the PRISM post-processor, statistical

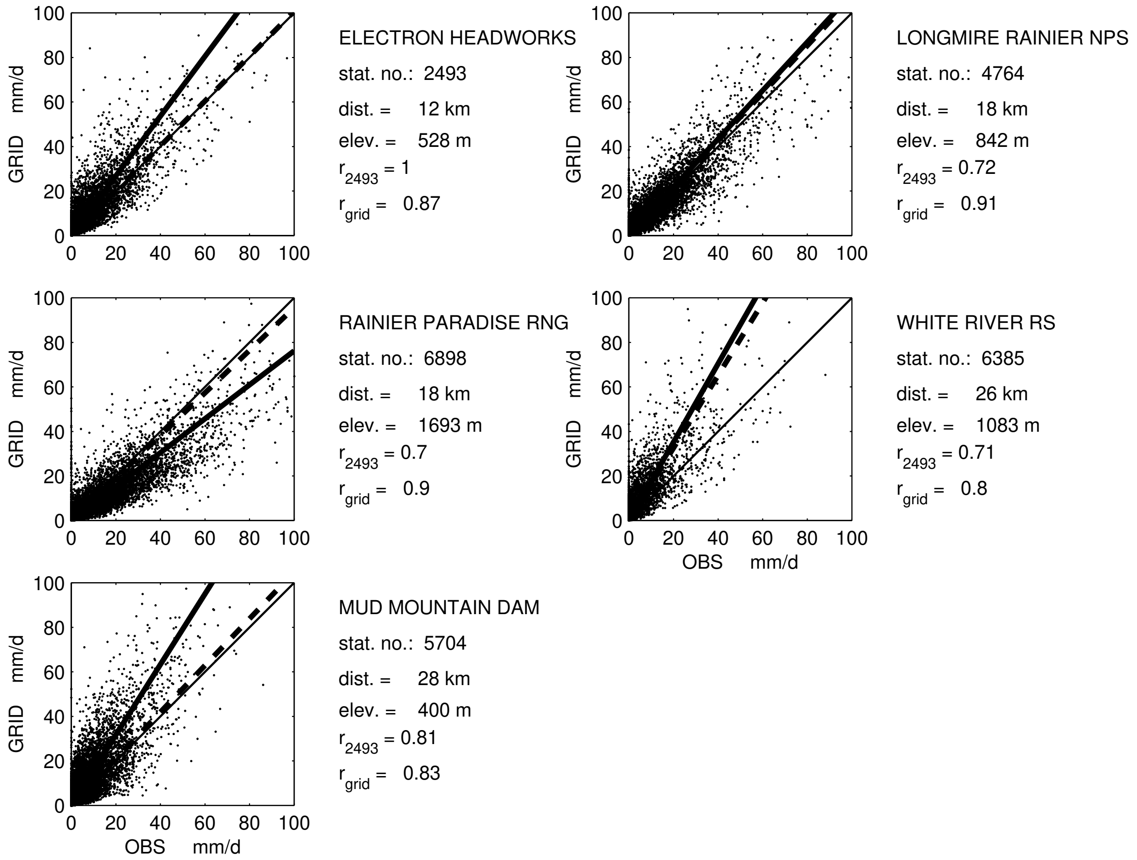

Figure 6: Daily precipitation at the grid cell containing Mt. Rainier (the cell is centered at 46.90 N and 121.87 W) versus the observations at the closest 5 stations. Station names, NCDC station numbers, distances to the center of the grid cell, and correlation coefficient with the record of Electron Headworks (closest to the center of the cell) and the grid cell series are indicated. The slope of the thick solid line is the average ratio of the grid-cell and the station series; for comparison the thin solid line depicts a ratio of 1. The dashed line shows the average ratio of a local precipitation estimate (discussed in section 2.4) and the station series.

stability of the regressions, and validation.

Here we propose an alternative and considerably simpler method. The full-resolution (4 km $\times$ 4 km) PRISM climatologies provide topography-based, small-scale information for long-term monthly means. So far we have only made use of their average over the 50 km grid cells. We can exploit the full information of these climatologies if we consider the decomposition of the precipitation field in a climatology $\overline{\psi}$ and a time-varying ratio field ψ_r (Eqn. 1) , use the already calculated ψ_r with the 50 km $\times$ 50 km resolution, but now multiply ψ_r with the PRISM climatologies given on the 4 km $\times$ 4 km grid.

This approach implies the assumption that the fine structure of precipitation within the 50 km cells of our data set is at any given day proportional to that of the full-resolution monthly PRISM fields and that all we can know about the temporal variability is

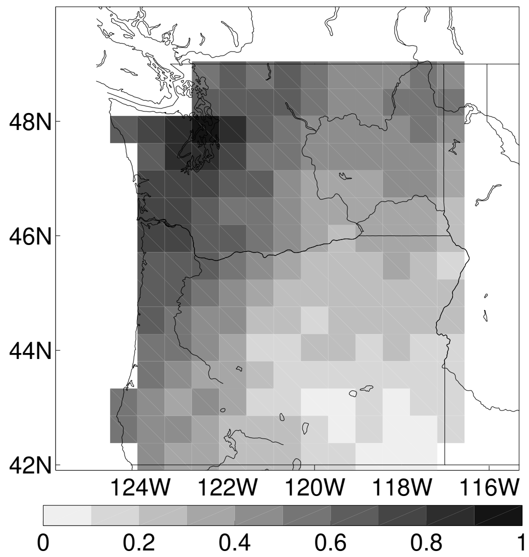

Figure 7: Correlation map of gridded daily precipitation series. The reference grid cell in northwestern Washington contains Seattle.

completely included in the 50 km field. For each day the average of the high-resolution data set over the 50 km grid cells is identical to the 50 km data set and the long-term monthly means of the high-resolution data are consistent with the respective PRISM climatologies. It has to be kept in mind that the temporal variance of individual normalized records is different from that of the grid-cell means ψ_r. Assuming a mean interstation correlation of 0.8 and equal weights for all stations, it follows from Eqn. 7 that the underestimation of the local variance varies between about 13% and 20% depending on the number of stations which were interpolated.

We can test this method by comparing the local series with station records. According to Daly et al. (1994) the correlation between precipitation and elevation is best for spatial scales around 4 km, and therefore the long-term mean of the local estimates should agree with that of the stations located within a given 4 km cell. The slope of the dashed line in Fig. 6 is the average ratio of local estimates and station records. For all stations but White River RS the average amount of local precipitation is almost perfectly estimated. The large deviation at White River RS can either be due to particular conditions at this station which make it nonrepresentative for the respective 4 km cell (in particular it is in the rain shadow of Mt. Rainier), or reflect deficiencies in the PRISM fields.

In order to omit the storage of redundant information, we did not calculate the high-resolution fields. Potential users should get the 50 km-resolution ψ_r from our web site (http://tao.atmos.washington.edu/data_sets/), the PRISM fields from the PRISM web site (http://www.ocs.orst.edu/prism/prism_new.html), and then perform the multiplication, segregated by the month of the year, for their specific area of interest.

3 Validation of reanalyzed precipitation

Here we compare the simulated precipitation from the NCEP reanalysis with the gridded precipitation data set presented above. For most of the validation the whole overlap period 1958-1994 is used. The reanalyzed precipitation is given on a T62 gaussian grid, which has a resolution of about $1.9^\circ \times 1.9^\circ$ or 210 km (lat) $\times$ 150 km (lon) at 45°N. The 52.5 km $\times$ 50 km grid for the daily observed precipitation is a subgrid of the reanalysis grid and area means with respect to the coarser grid are obtained by averaging over 12 cells of the finer grid (cf. Fig. 1). For the reanalysis cells at the western and northern boundaries of the analysis domain the averaging of gridded observations was done over all subcells which were available (at least 8). All analyzed reanalysis cells are classified as land.

3.1 Bias and seasonal cycle

Like the high-resolution climatology in Fig. 5a, the observations in Fig. 8 show large gradients of annual precipitation means across the Cascade Mountains. Since the NCEP model topography (not shown) does not resolve this mountain range, it can be expected that the reanalysis does not reproduce these gradients. In fact, Fig. 8 shows that the reanalyzed precipitation is too low to the west of the main crest and too high to the east. The area mean with respect to the entire analysis region agrees well with observation, the ratio between reanalyzed and observed averages over all 15 grid cells is 0.94. As discussed above, estimates for the annual-mean undercatch range from 6% for coastal regions to 20% for high elevations, and an undercatch correction could therefore slightly alter the results of this comparison.

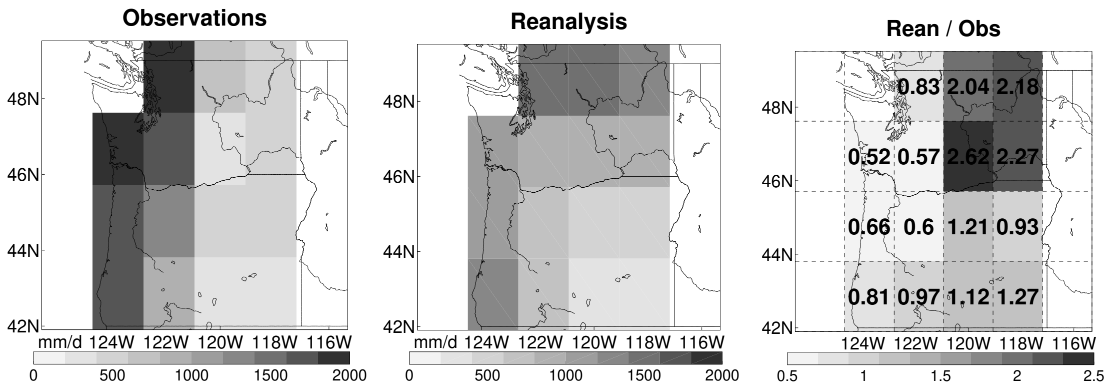

Figure 8: Observed and reanalyzed annual mean precipitation for the period 1958-1994. The third panel depicts the ratio.

The annual cycle of precipitation is depicted in Fig. 9. We selected two adjacent grid cells in southern Washington where the ratios between reanalyzed and observed long-term annual means are particularly low and high. During the whole year the reanalysis is too dry in the cell west of the Cascades and too wet to the east. The reanalyzed/observed precipitation ratio for the western cell varies between 0.4 in October and 0.85 in March, and for the eastern cell between 4.5 in April and 2 in August. The annual cycles of the ratio at the two cells (not shown) are almost proportional and indicate relatively wet conditions in the reanalysis between March and July. Long-term monthly means of total precipitation over Oregon and Washington are well reproduced by the reanalysis. The ratio varies from about 0.75 for August to October up to about 1.25 for April to June.

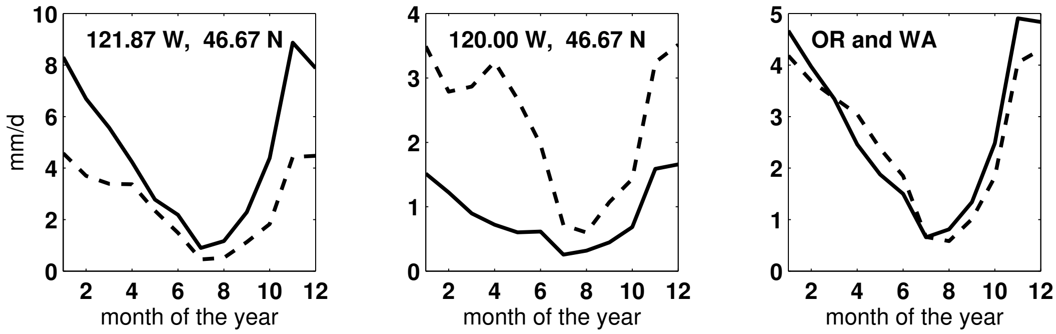

Figure 9: Observed (solid lines) and reanalyzed (dashed lines) long-term monthly precipitation means (1958-1994) at two grid cells west (left panel) and east (middle panel) of the Cascade Mountains, and for all 15 grid cells covering Oregon and Washington.

3.2 Temporal variability

We now investigate to what degree the temporal variability of precipitation is reproduced in the reanalysis. Our main focus is on the component of temporal variability that is not part of the pronounced seasonal cycle. Unless stated otherwise, correlation coefficients for daily and monthly data are based on normalized records. At each grid cell we divide the observed and reanalyzed series by their respective long-term (1958-1994) monthly means. If one actually were to estimate precipitation from the reanalysis, one would use the knowledge of the biases discussed above to correct the simulated precipitation. Debiased reanalyzed precipitation can be obtained by multiplying the reanalyzed precipitation, individually for each grid cell and each month of the year, by the ratio of the observed and reanalyzed long-term means (1958-1994). In general the correlations of debiased reanalysis values and observations can be expected to be higher than the correlations of normalized series, because the former still include the seasonal cycle.

Daily normalized precipitation for a randomly selected period at the same two grid cells as in Fig. 9 is shown in Fig. 10. The observations are similar on the two sides of the Cascade Mountains and the wet and dry spells are accurately reproduced in the reanalysis, although on some days there are considerable differences in the amounts of observed and reanalyzed normalized precipitation. The correlations of daily normalized values at each grid cell are presented in the left hand panel of Fig. 11. Maximal values up to 0.77 are found along the coast, minimal values down to 0.54 are obtained east of the Cascades.

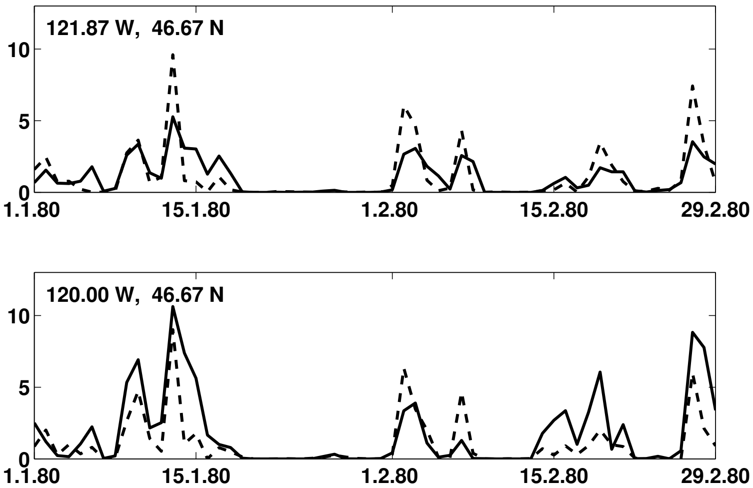

Figure 10: Daily precipitation Jan. 1980 - Feb. 1980 at the same grid cells as in Fig. 9. Solid lines: ratio of daily observed precipitation and the observed long-term monthly mean; dashed lines: ratio of reanalyzed daily precipitation and the reanalyzed long-term monthly mean. Correlations with respect to 1958 - 1994 (as in Fig. 11, left panel) are 0.73 (upper panel) and 0.54 (lower panel).

Monthly normalized values yield higher correlations (Fig. 11, middle panel) and the spatial pattern remains almost unchanged. Again, the highest correlations, up to 0.87, are located along the coast, while the lowest value of 0.68 is obtained to the east of the Cascades at the same grid cell as for daily correlations. An example for the time series of normalized monthly precipitation is given in Fig. 12. The first two panels refer to the same grid cells as above. The lower panel depicts normalized total precipitation over Oregon and Washington (long-term monthly means for the entire area have been used for normalization). Correlations between non-normalized annual means (Fig. 11, right panel) to the east of the Cascades are smaller than those for monthly means; the minimum value is now 0.33. In the western part they are are similar to the monthly-mean correlations. The correlation with respect to total annual precipitation over Oregon and Washington is 0.83.

Seasonally segregated data yield a similar spatial dependence of the correlations (not shown). Daily normalized data show moderate seasonal effects on both sides of the Cascades, with lowest skill of the reanalysis in summer (0.48 - 0.73) and highest in fall (0.59 - 0.82) and winter (0.59 - 0.83) . Correlations of monthly normalized data show a more pronounced seasonal cycle to the east of the Cascades with a minimum in spring (minimum 0.52) and maximum in fall (minimum 0.72). To the west, the correlations are high during the entire year (maximum 0.86 (JJA) - 0.93 (DJF)). Normalized total precipitation over the entire analysis domain is dominated by the wet areas in the west and the respective correlations consequently show only a weak seasonality (0.88 (JJA) - 0.96 (SON)).

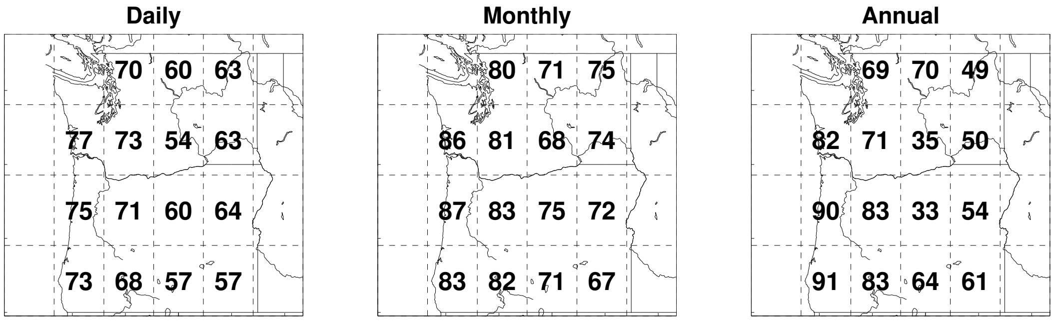

Figure 11: Correlations between observed and reanalyzed precipitation. Daily and monthly grid-cell series are normalized, i.e. observed and reanalyzed values are divided by their respective long-term monthly means. Annual means are used directly.

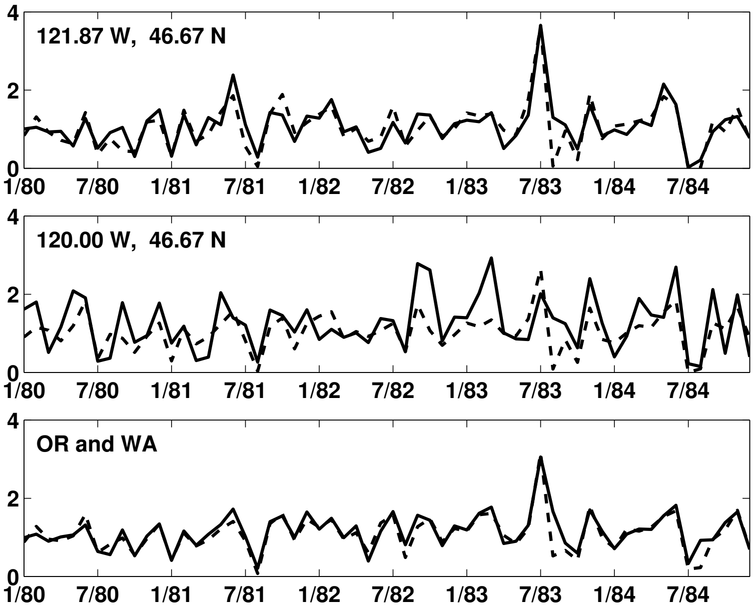

Figure 12: Normalized monthly precipitation Jan. 1980 - Dec. 1985 at the same grid cells as in Figs. 9 and 10 and for total precipitation over Oregon and Washington. Correlations with respect to 1958 - 1994 (as in Fig. 11, middle panel) are 0.81 (upper panel) and 0.68 (middle panel), for total precipitation over Oregon and Washington it is 0.90.

We also calculated the correlations of observations and debiased monthly means from the reanalysis. Total debiased precipitation over Oregon and Washington was obtained by summing the debiased monthly means at all grid cells rather than defining monthly correction factors valid for the whole region. Since the seasonal cycle is still important within the 3 month periods, most correlations are higher than for normalized data. The minima are still to the east of the Cascades (0.58 (MAM) - 0.82 (SON)). To the west, correlations of monthly means are high for all seasons (maximum 0.90 (JJA) - 0.95 (SON)), as they also are for total precipitation (0.92 (JJA, MAM) - 0.97 (SON)). The annual mean of the debiased total precipitation is only slightly better correlated with observations than the reanalyzed annual mean (0.84 instead of 0.83).

3.3 Intensity distributions

Saturation of soil with water, river discharges, floodings, landslides and many other processes are particularly sensitive to extreme values of precipitation. We now examine how well the frequency distribution of daily precipitation is reproduced in the reanalysis. For this analysis it is particularly important that the temporal variances of the area means over a reanalysis grid cell are correctly estimated from the station records. Again we use Eqn. 7 to roughly asses the degree of overestimation. We assume that averaging the 12 area means from the 50 km grid which are located in a reanalysis grid cell, basically yields an average over all stations in in the reanalysis cell. The average number of stations per cell is about 22. Since the area is now larger than for similar estimations performed above for the 50 km grid, we use a lower mean interstation correlation of 0.7. It follows from these numbers that the overestimation of the temporal variance of the area mean over a NCEP cell is smaller than 2% and therefore negligible.

Since the systematic biases of the reanalysis will be corrected in typical applications, we compare the cumulative distribution function of debiased reanalyzed daily precipitation with observations. The first two panels of Fig. 13 refer to the same grid cells as in Figs. 9, 10 and 12. A comparison of the observed distribution on the 50 km grid with that on the larger grid reveals, at both cells, the broadening of the distribution with higher resolution. To the west of the Cascades the reanalysis slightly overestimates the number of dry days which were observed and follows the observed cumulative distribution function closely for medium to high values of precipitation. To the east the intensity distribution of the reanalysis is somewhat narrower than that of the observations. However, for both cells the differences are small and debiased reanalyzed precipitation exhibits very realistic intensity distributions. We carefully compared the probability distribution functions for high intensity precipitation and found an excellent agreement between observations and reanalysis to the west of the Cascades and for the 2 cell mean and a slight underestimation in the reanalysis for the eastern grid cell. Since the Cascade Mountains do not exist in the reanalysis GCM, the distribution of reanalyzed precipitation (without debiasing) at the two cells is almost identical. It follows that the effect of the Cascades on the observed distribution function is mainly a scaling of the values. If we average over the two grid cells the debiased reanalysis and the observations agree almost perfectly (right hand panel).

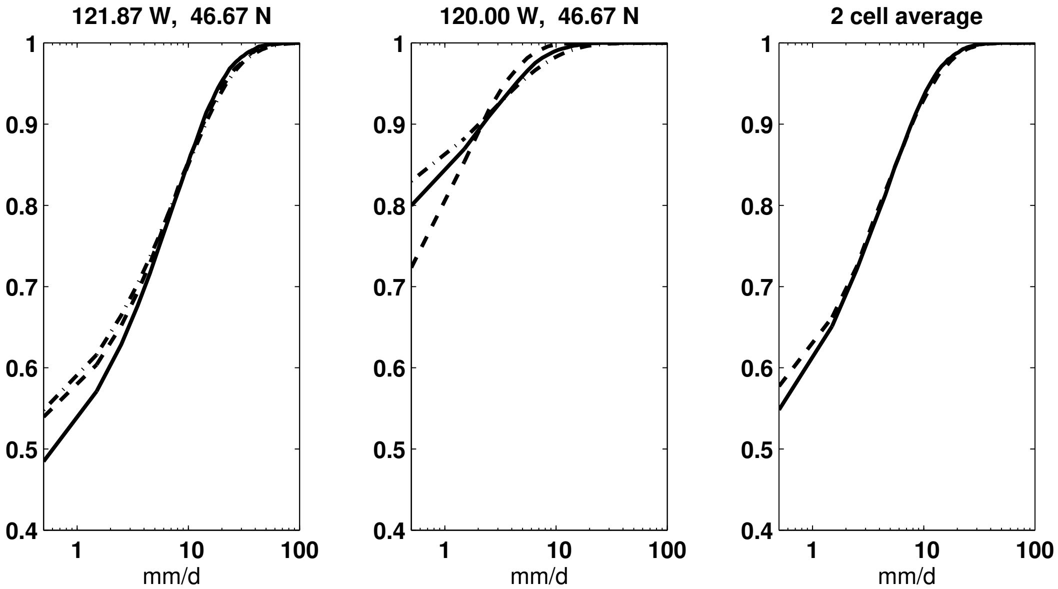

Figure 13: Cumulative frequency distribution (CDF) of observed (solid lines) and debiased reanalyzed (dashed lines) daily precipitation at two grid cells (same as in Figs. 9, 10 and 12). The right hand panel shows the CDF for the average over both cells. The one-cell panels include in addition the CDF of observed daily precipitation at all 50 km cells within the reanalysis cells (dashed-dotted lines).

4 Discussion and conclusions

We compiled a daily precipitation data set for the period 1949-1994 over Oregon and Washington on a regular grid with about 50 km resolution. It is based on a large number of daily station records and on long-term monthly PRISM climatologies. Our gridding procedure estimates area means and includes the influence of topography on precipitation. Many problems in fields such as hydrology, precipitation climatology, modeling of ecosystems, statistical downscaling, or validation of numerical models may be better addressed using these area means rather than station records. We also demonstrated how to estimate daily precipitation on a grid with 4 km resolution. Our data set is available for potential users on the internet (http://tao.atmos.washington.edu/data_sets/) and written in a standard format (netCDF).

These data were compared with the precipitation simulated in the NCEP reanalysis. The underlying question is how well GCMs can simulate regional precipitation over complex terrain if the synoptic-scale pressure, temperature and humidity is accurately represented in the simulation. It is known from earlier studies that the correlation between reanalyzed and observed precipitation shows a strong regional dependence, and, strictly interpreted, our results hold for the Pacific Northwest and the NCEP model only. A generalization of our results may be justified to GCMs with similar precipitation physics and resolution, and to other regions where previous large-scale studies indicated that the reanalysis matches the observations well. These include many midlatitude regions where cyclones and their associated fronts, moisture advection and orographic lifting are the main factors determining the precipitation climate. The model skill is usually lower in regions which are dominated by convective processes or local water cycles.

As expected, the coarse GCM topography, which does not represent the local mountain ranges, leads to differences between reanalyzed and observed long-term precipitation means on the scale of individual grid cells. The long-term monthly means of total precipitation over Oregon and Washington, i.e. over a spatial scale of about 3 grid cells, are well simulated. Temporal variability is surprisingly well represented in the reanalysis even at individual cells. To the west of the Cascades, debiased reanalyzed monthly means are highly correlated (about 0.9) with observations in all seasons. To the east, these correlations are still high and range from about 0.6 to 0.8. Correlations of annual means range from 0.91 to 0.35. Intensity distribution functions of debiased daily values are very realistic. Thus the NCEP GCM can provide useful information about daily to interannual variability of precipitation at individual grid cells.

The estimation of decadal-scale precipitation variability with reanalysis data merits an additional cautionary comment. A method that satisfactory estimates month-to-month variations does not necessarily reproduce decadal-scale variations and long-term trends. This problem may seriously limit the realism of precipitation scenarios produced by means of statistical or numerical methods (Widmann and Schär 1997; Wilby 1997, 1998). Analyzing long-term variability requires data that are very carefully checked for temporal homogeneity, which is not the case for all of the NCDC station records used in our analysis. Therefore we tested the ability of the NCEP reanalysis to reproduce long-term precipitation variability with respect to the well examined (Widmann and Schär, 1997) and large wintertime trends in Switzerland (approx. +20% for DJF 1961-1990). Although the correlations of reanalyzed and observed monthly means are also high for Switzerland (around 0.75) there is no substantial positive trend in reanalyzed precipitation for this period.

How well reanalyzed precipitation compares to precipitation estimates derived from statistical downscaling methods is an important and open question, which will be addressed in a future study. Since the good skill of the reanalysis might be partly due to the fact that assimilated humidity fields enter the calculation of precipitation, we will not only use synoptic-scale pressure and temperature, but also humidity as a predictor in the statistical downscaling. We will also investigate whether the results of statistical downscaling techniques can be improved if simulated precipitation is used as a predictor.

A prerequisite for the high skill of the reanalysis GCM in simulating precipitation is the exact representation of the synoptic-scale variables. This would not be a given if this GCM was not constrained by atmospheric observations (as in the reanalysis), but forced by sea surface temperatures (as for seasonal forecast) or changing CO_2 concentrations (as in climate change experiments). Notwithstanding this important caveat, our findings are still relevant in these cases, because they suggest that the simulated precipitation, although not realistic, would be consistent with the simulated synoptic-scale states (to the extent given by our analysis). Note in this context that alternative methods of estimating precipitation from synoptic-scale variables, namely statistical downscaling or the use of regional numerical models, also rely on realistic input fields. Errors in GCM-simulated synoptic-scale fields are propagated by any method.

Acknowledgments. This research was supported by the National Science Foundation (NSF) under Grant DMS-9524770. The first author was also supported by a grant from the Swiss National Science Foundation. We are indebted to the National Climate Data Center (NCDC) for permissions to use their precipitation records and to Christopher Daly for comments and for providing the PRISM climatologies. NCAR/NCEP Reanalysis data were provided through the NOAA Climate Diagnostics Center (http://www.cdc.noaa.gov/). We are grateful for many valuable comments and technical support to Michela Biasutti, Christoph Frei, Dennis Lettenmaier, Todd Mitchell, Bart Nijssen, Christoph Schär and to two anonymous reviewers.

References

Busuioc, A., H. von Storch and R. Schnur, 1999: Verification of GCM-generated regional seasonal precipitation for current climate and of statistical downscaling estimates under changing climate conditions. *J. Clim.*, **12**, 258-272.

Daly, C., R. P. Neilson and D. L. Phillips, 1994: A statistical-topographic model for mapping climatological precipitation over mountainous terrain. *J. Appl. Met.*, **33**, 140-158.

Daly, C., G. Taylor and W. Gibson, 1997: The PRISM approach to mapping precipitation and temperature. *Proc. 10th Conf. on Applied Climatology*, Reno, NV, Amer. Meteor. Soc., 10-12.

EarthInfo Inc., 1996: NCDC Summary of the Day. [Avail. from EarthInfo Inc., 5541 Central Avenue, Boulder, CO 80301].

Frei, C. and C. Schär, 1998: A precipitation climatology of the Alps from high-resolution rain-gauge observations. *Int. J. Climatol.*, **18**, 873-900.

Groisman, P. Y. and D. R. Legates, 1994: The accuracy of the United States precipitation data. *Bull. Amer. Met. Soc.*, **75**, 215-227.

Gutowski, W. J. (jr), Y. Chen, and Z. Ötles, 1997: Atmospheric Water Vapor Transport in NCEP-NCAR Reanalyses: Comparison with river discharge in the Central United States. *Bull. Amer. Met. Soc.*, **78**, 1957-1969.

Higgins, R. W., K. C. Mo and S. D. Schubert, 1996: The moisture budget of the central United States as evaluated in the NCEP/NCAR and the NASA/DAO reanalyses. *Mon. Wea. Rev.*, **124**, 939-963.

Huffman, G. J., R. F. Adler, P. A. Arkin, A. Chang, R. Ferraro, A. Gruber, J. Janowiak, R. J. Joyce, A. McNab, B. Rudolf, U. Schneider and P. Xie, 1997: The Global Precipitation Climatology Project (GPCP) combined precipitation data set. *Bull. Am. Met. Soc.*, **77**, 5-20.

Hulme, M., D. Conway, P. D. Jones, T. Jiang, E. M. Barrow and C. Turney, 1995: Construction of a 1961-1990 European climatology for climate change modelling and impact applications. *Int. J. Climatol.*, **15**, 1333-1363.

Janowiak, J. E., A. Gruber, C. R. Kondragunta, R. E. Livezey and G. J. Huffman, 1998: A comparison of the NCEP-NCAR Reanalysis precipitation and the GPCP rain gauge-satellite combined dataset with observational error considerations. *J. Clim.*, **11**, 2960-2979.

Kagan, R. L., 1966: *An evaluation of the representativeness of precipitation data* (in Russian). Gidrometeoizdat.

Kalnay, E., M. Kanamitsu, R. Kistler, W. Collins, D. Deaven, L. Gandin, M. Iredell, S. Saha, G. White, J. Woollen, Y. Zhu, M. Chelliah, W. Ebisuzaki, W. Higgins, J. Janowiak, K. C. Mo, C. Ropelewski, J. Wang, A. Leetmaa, R. Reynolds, R. Jenne and D. Joseph, 1996: The NCEP/NCAR reanalysis project.. *Bull. Amer. Meteor. Soc.*, **77**, 437-471.

Lau, K.-M., J. H. Kim and Y. Sud, 1996: Intercomparison of hydrologic processes in AMIP GCMs. *Bull. Amer. Meteor. Soc.*, **77**, 2209-2227.

Legates, D. R. and C. J. Willmott, 1990: Mean seasonal and spatial variability in gauge-corrected, global precipitation. *Int. J. Climatol.*, **10**, 111-127.

Legates, D. R. and T. L. DeLiberty, 1993a: Estimates of biases in precipitation gage measurements: An example using the United States raingage network. *Proc. Eigth Symposium on Meteorological Observations and Instrumentation*, Anaheim, CA, Amer. Meteor. Soc., J48-J51.

Legates, D. R. and T. L. DeLiberty, 1993b: Measurement biases in the United States raingage network. *Proc. Symposium on Geographic Information Systems and Water Resources*, Mobile, AL, AAG, 547-557.

Leung, L. R. and S. J. Ghan, 1999: Pacific Northwest climate sensitivity simulated by a regional climate model driven by a GCM. Part I: Control simulations. *J. Clim.*, in press.

Mo, K. C. and R. W. Higgins, 1996: Large-scale atmospheric moisture transport as evaluated in the NCEP/NCAR and the NASA/DAO reanalyses. *J. Clim.*, **9**, 1531-1545.

Neff, E. L., 1977: How much rain does a rain gage gage? *J. Hydrology*, **35**, 213-220.

New, M., M. Hulme and P. D. Jones, 1999: Representing twentieth century space-time climate variability. Part 1: development of a 1961-90 mean monthly terrestrial climatology. *J. Clim.*, **12**, 829-856.

Nijssen, B., D. P. Lettenmaier, X. Liang, S. W. Wetzel, and E. F. Wood, 1997: Streamflow simulation for continental-scale river basins. *Water Resources Res.*, **33**(4), 711-724.

Osborn, T. J. and Hulme, M., 1997: Development of a relationship between station and grid-box rainday frequencies for climate model evaluation. *J. Clim*, **10**, 1885-1908.

Osborn, T. J. and Hulme, M., 1998: Evaluation of the European daily precipitation characteristics from the atmospheric model intercomparison project. *Int. J. Climatol.*, **18**, 505-522.

Osborn, T. J., D. Conway, M. Hulme, J. M. Gregory and P. D. Jones, 1999: Air flow influences on local climate: observed and simulated mean relationships for the United Kingdom. *Clim. Res.*, accepted.

Raulin, V., 1879: Über die Vertheilung des Regens im Alpengebiet von Wien bis Marseille. *Zeitschrift der österreichischen Gesellschaft für Meteorologie*, **14**, 233-247.

Risbey, J. S. and P. H. Stone, 1996: A case study of the adequacy of GCM simulations for input to regional climate change assessments. *J. Clim*, **9**, 1441-1467.

Rudolf, B., H. Hauschild, W. Rüth and U. Schneider, 1994: Terrestrial precipitation analysis: Operational method and required density of point measurements. In *Global Precipitations and Climate Change*, Eds. M. Desbois and F. Desalmond, NATO ASI Series I, 26, Springer-Verlag, 173-186.

Rudolf, B., H. Hauschild, W. Rüth and U. Schneider, 1996: Comparison of raingauge analyses, satellite-based precipitation estimates and forecast model results. *Adv. Space. Res.*, **7**, 53-62.

Sevruk, B., 1982: Methods of correction for systematic error in point precipitation measurement for operational use. Operational Hydrology Report No. 21, World Meteorological Organisation, Geneva, WMO No. 589, 91 pp.

Shepard, D. S., 1968: A two-dimensional interpolation function for irregularly spaced data. *Proc. 23rd Association for Computing Machinery Conference*, Brandon/System Press, Inc., Princeton, NJ, 517-524.

Shepard, D. S., 1984: Computer Mapping: The SYMAP interpolation algorithm. In *Spatial Statistics and Models*, Eds. Gaile G. L. and C. J. Willmott, D. Reidel Publishing, Dordrecht, Holland, 133-145.

Skelly, W. C. and A. Henderson-Sellers, 1996: Grid-box or grid-point: what type of precipitation data do GCMs deliver? *Int. J. Climatol.*, **16**, 1079-1086.

Stendel, M. and K. Arpe, 1997: Evaluation of the hydrological cycle in reanalyses and observations. ECMWF Re-Analysis Validation Reports - Part 1. ECMWF Re-Analysis Project Report Series, 6, 53 pp.

Vogel, R. M. and J. R. Stedinger, 1985: Minimum variance streamflow augmentation procedures. *Water Resources Res.*, **21**, 5, 715-723.

Widmann, M. and C. Schär, 1997: A principal component and long-term trend analysis of daily precipitation in Switzerland. *Int. J. Climatol.*, **17**, 1333-1356.

Wilby, R. L., 1997: Nonstationarity in daily precipitation series: implications for GCM downscaling using atmospheric circulation indices. *Int. J. Climatol.*, **17**, 439-454.

Wilby, R. L., 1998: Statistical downscaling of daily precipitation using airflow and seasonal teleconnection indices. *Clim. Res.*, **10**, 163-178.

Wilby, R. L. and Wigley, T. M. L., 1999: Precipitation predictors for downscaling: observed and general circulation model relationships. *Int. J. Climatol.*, submitted.

Willmott, C. J., C. M. Rowe and W. D. Philpot, 1985: Small-scale climate maps: A sensitivity analysis of some common assumptions associated with grid-point interpolation and contouring. *The American Cartographer*, **12**(1), 5-16.